Challenge Journal of Structural Mechanics

Modelling of non-linear seismic ground response using elasto-plastic constitutive framework within a finite element soil column model

Azeddine Chehat [a], Zamila Harichane [b,*], Amina Sadouki [b]

[a] *Department of Civil Engineering, University Djilali Bounaama, 44000 Khemis Meliana, Algeria*
[b] *Geomaterials Laboratory, University Hassiba Benbouali of Chlef, 02000 Chlef, Algeria*

ABSTRACT

The prediction of seismic ground response is conditioned by the knowledge of each material behavior of soil deposits. The recourse to plasticity criterion to simulate cyclic behavior of soils under seismic loading is becoming more realistic. In this study, an elasto-plastic constitutive equation is cast within the framework of one dimensional finite element (FE) soil column model to account for the spatial and material nonlinearity of the secant shear modulus. To account of the spatial non linearity, shear modulus is written in terms of rigid base shear modulus and height of the soil column, while for material nonlinearity, the shear modulus degradation is deducted by the application of the isotropic evolution of the Von Misès criterion. Obtained results proved the efficiency of the proposed methodology and the predictive capability of the elaborated elastoplastic model which captures both small- and large-strain behaviors. They likewise highlight the important roles that play the spatial and material shear modulus variation in the prediction of the seismic soil responses.

ARTICLE INFO

Article history:
Received 26 January 2017
Revised 25 April 2017
Accepted 13 May 2017

Keywords:
Von Misès criterion
Cyclic behaviour
Shear modulus
Seismic response
Bessel's function
Large-strain

1. Introduction

Under seismic loadings, soil behavior is highly nonlinear. For this kind of loading, the soil behaves strongly non-linear due to the degradation of the shear modulus (Mercado et al., 2015). So, adequate constitutive equation should be used to accurately predict the nonlinear soil behavior. For several decades, the soil behavior under different loading conditions was satisfactorily studied by numerical methods, particularly by the finite element method (FEM). The one-dimensional (1-D) modelling of soil profiles by the FEM under cyclic loading was widely used by several researchers (Hashash and Park, 2002; Stewart et al., 2008; Vasileios et al., 2012; Kaklamanos et al., 2015; Mercado et al. 2015)

The prediction of the nonlinear response depends on several factors such as geotechnical data, especially the variation of shear modulus, and the mathematical model chosen to describe the stress-strain relationship (τ-γ). Harichane et al. (2011a) used a 1-D Finite Elements (FE) model to describe the nonlinear behavior of geomaterials under seismic loads. The 1-D FE model was validated by Harichane et al. (2011b) using seismic data recorded during the 2003 Boumerdes earthquake (M=6.9), deeply studied by Khellafi et al. (2013), and soil profile's characteristics identified by an inverse analysis carried by Harichane et al. (2012).

The nonlinear soil responses may be mainly predicted in terms of accelerations, velocities, displacements, strain, and stresses. This response can be obtained at any depth of a soil profile by considering spatial and material variation of shear modulus. The last one is commonly represented in puissance description (Abdelghaffar and Koh, 1981). However, there is not a universal constitutive equation to describe the behavior of the soils under any kind of excitations but some ones exist in literature for specified materials.

The present study is mainly intended to carry out an efficient methodology to predict the nonlinear cyclic response of a soil profile using the FEM together with the Von Misès elasto-plastic criterion. A simple case study concerned with the behavior a soil profile excited at its

* *Corresponding author*. Tel.: +213-027-776398 ; Fax: +213-027-721794 ; E-mail address: zharichane@gmail.com (Z. Harichane)
ISSN: 2149-8024 / DOI: https://doi.org/10.20528/cjsmec.2017.05.011

rigid base by a first order Ricker signal is carried out. The spatial variation of the shear modulus is captured by an exponential expression depending on the height and the shear modulus at the base of the soil profile. A 1-D FE model is translated in a computer program, in the MATLAB environment, incorporating the Von-Misès criteria with a linear hardening in both small- and large-strain analyses. The dynamic governing equation is solved by Newmark's non-linear integration with modified Newton's iteration, detailed in (Bathe, 1996).

Results are obtained in terms of depth-dependent distribution of maximum displacement, depth-dependent distribution of maximum acceleration with respect to that at the base of the soil profile, and stress-strain hysteretic loop, where the effect of spatial and material non-linearity of shear modulus as well as small- and large-strain assumptions are examined.

2. Basic Equations

The forces acting on a soil element with dimensions (dx, dy, dz) in a soil profile (Fig. 1) are: *(i)* the inertia force (F_I), *(ii)* the shearing force (S_{xy}), and *(iii)* the earthquake force (F_g), given, respectively, by Eqs. (1) to (3).

$$F_I = \rho dxdydz.\ddot{u}(x,y,t)\,, \tag{1}$$

$$S_{xy} = dxdz.\frac{\partial\tau_{xy}(y,t)}{\partial y}\,, \tag{2}$$

$$F_g = \rho dxdydz.\ddot{u}_g(t)\,, \tag{3}$$

where ρ is the mass density of the soil element, $\partial\tau_{xy}(y,t)/\partial y$ the variation of the shear stress in the soil element due to a base shear motion $\ddot{u}_g(t)$, and $\ddot{u}(x,y,t)$ the soil element acceleration. The equations of motion of the soil element is then;

$$\rho.\ddot{u}(x,y,t) = \frac{\partial\tau_{xy}(y,t)}{\partial y} - \rho\ddot{u}_g(t)\,. \tag{4}$$

The original displacement is represented by nodal displacements and the stresses are interpreted by the associated nodal forces. The governing equation of motion is described for the j^{th} step as (Elgamal, 1991; Gu et al., 2009; Hashash and Park, 2001).

$$[M]\{\Delta\ddot{u}\}_j + [C]_j\{\Delta\dot{u}\}_j + \int_\Omega [B]_j^T\{\Delta\sigma\}_j d\Omega = -[M]\{\Delta\ddot{u}_g\}\,. \tag{5}$$

In Eq. (5), $[\mathrm{B}]_j^T$ defines the displacement-strain matrix. [M] and $[\mathrm{C}]_j$ denote the mass and damping matrices, respectively. The damping matrix $[\mathrm{C}]_j$ is proportional to the mass and the stiffness matrices.

$$[C]_j = \alpha_1[M] + \alpha_2[K]_j\,, \tag{6}$$

where α_1 and α_2 are coefficient to be determined (Harichane et al., 2011b; Chopra, 2012).

The time domain step-by-step solution of the semi-discrete matrix equation (5) is performed using the Newmark family methods (Bathe, 1996). From Eq. (5), the material or kinematic nonlinearity occurs in the internal forces $\int_\Omega [\mathrm{B}]_j^T\{\Delta\sigma\}_j d\Omega$ that depends on the elasto-plastic stress $\{\Delta\sigma\}_j$ (Dunne and Petrinic, 2006).

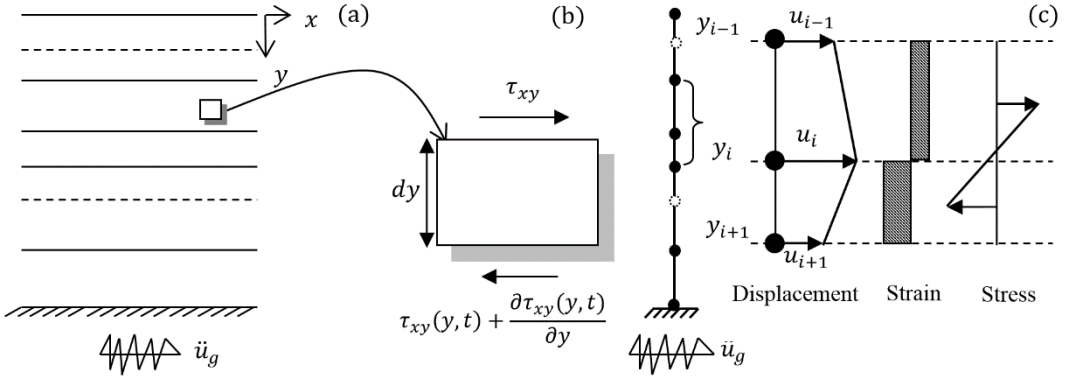

Fig. 1. Schematization of: (a) soil profile; (b) stress acting on a soil finite element; and (c) discrete model with details illustrating the definition of displacement, strain and stress.

3. Free Vibrations

An essential step in the determination of the damping matrix (Eq. (6)), is the calculation of the natural frequencies. In this way, the equation of motion in free vibration, also called wave equation, is solved using Bessel's functions as usually done in such problems. Citing, without exclusivity, the work of Pecker (1995) in which eigenfrequencies of a soil profile with shear wave velocity varying in power exponent (B) of depth were obtained using Bessel's function of order *(B-1)/(2-B)* and validated experimentally. Similarly, Afra and Pecker (2002) solved the wave equation for a soil deposit with shear modulus increasing with power exponent of depth to obtain the surface spectrum derived from an accelerogram compatible with the Eurocode 8 response spectrum.

In the present study, the linear elastic shear stress-strain response is expressed by

$$\tau_{xy}(y,t) = G(y)\frac{\partial u(x,y,t)}{\partial y}\,. \tag{7}$$

In Eq. (7), $\partial u(x,y,t)/\partial y$ is the shear strain and $G(y)$ the shear modulus of non-homogeneous soil profile assumed in the following form (Elgamal, 1991; Dakoulas and Gazetas, 1985).

$$G(y) = G_b(\frac{y}{h})^B \,, \tag{8}$$

where G_b is the shear modulus at the base of the soil profile, h its height and $0 \leq B \leq 1$.

A solution of the eigenvalue problem which corresponds to Eq. (5) may be obtained by setting

$$u(y,t) = \psi(y)e^{i\omega t} \,, \tag{9}$$

which yields to the following Bessel's equation.

$$y^2\frac{d^2\psi}{dy^2} + By\frac{d\psi}{dy} + \frac{\rho\omega^2 h^B}{G_b}y^{2-B}\psi = 0 \,, \tag{10}$$

The solution of Eq. (10) may be obtained in the form of,

$$\psi = (y)^{\frac{1-B}{2}}\left[C_1 J_{\frac{(1-B)}{(2-B)}}(\frac{2}{(2-B)}\sqrt{\frac{\rho_i\omega^2 h^B}{G_b}}y^{(\frac{2-B}{2})}) + C_2 J_{-\frac{(1-B)}{(2-B)}}(\frac{2}{(2-B)}\sqrt{\frac{\rho_i\omega^2 h^B}{G_b}}y^{(\frac{2-B}{2})})\right], \tag{11}$$

while C_1 and C_2 are integration constants.

For a soil profile of thickness h, for which the shear wave velocity V is equal to V_b, it can be shown that the eigen frequencies are given by

$$\omega_i = \frac{a_i(2-B)}{2}\frac{V_b}{h} \,, \tag{12}$$

where the a_i values are the roots of frequency equation $J_{-\frac{(1-B)}{(2-B)}}(a_i) = 0$ which depend on the inhomogeneity B (Dakoulas and Gazetas, 1985).

The plots of the first kind of Bessel's function $J_0(\omega_i/2\pi)$, $J_{0.25}(\omega_i/2\pi)$, $J_{1/3}(\omega_i/2\pi)$, $J_{0.4}(\omega_i/2\pi)$ and $J_{0.5}(\omega_i/2\pi)$ are shown in Fig. 2 for different materials $(0 \leq B \leq 1)$. After Afra and Pecker (2002), many soil deposits undergo variation of shear modulus in the form of Eq. (8) such that for cohesionless materials the value of B varies from 0.45 to 0.6 while for normally consolidated clays B varies from 0.8 to 1.

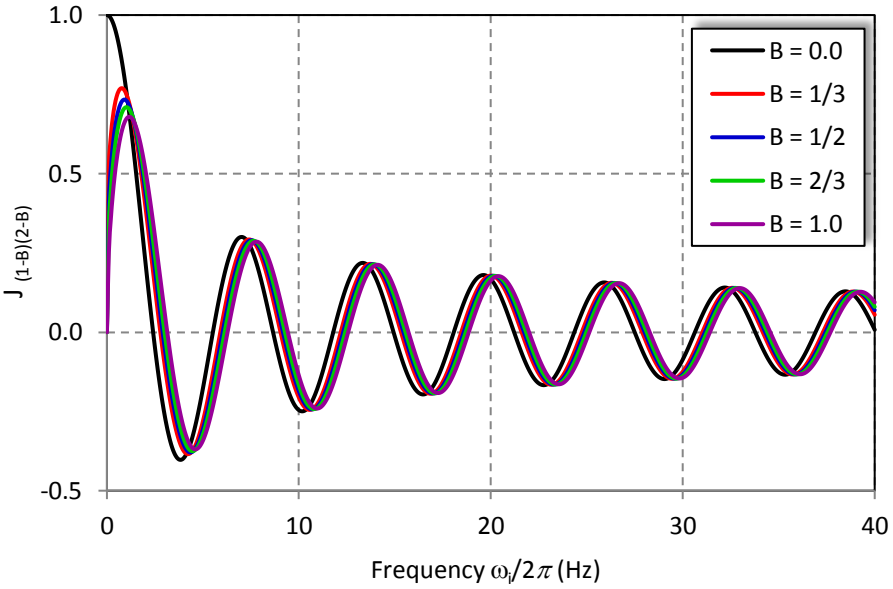

Fig. 2. Bessel' function of the first kind $J_{\frac{1-B}{2-B}}, B \in [0,1]$.

4. Integration of the Constitutive Equation for Material Nonlinearity

A one-dimensional elasto-plastic model based on the flow or incremental theory of plasticity according to Von-Misès criterion is used to describe the nonlinear hysteretic shear stress versus shear strain behavior of the soil material (Dunne and Petrinic, 2006). The constitutive equation is written in the following form.

$$f^{VM} = \sqrt{3J_2} - Y = 0 \,. \tag{13}$$

The parameter Y represents the size of the yield surface which defines the region of constant plastic shear modulus.The yield criterion determines the stress level at which plastic deformation begins and can be written in the general form (Fig. 3).

$$f(\tau, r) = 0 \,, \tag{14}$$

The consistency condition is written for an incremental change in stress and effective plastic strain $(f_{n+1}(\tau_{n+1}, \lambda_{n+1}) = 0)$ where $d\lambda$ is the plastic multiplier. This can be expanded as

$$f(\tau_{n+1}, \lambda_{n+1}) = f_n(\tau_n, \lambda_n) + \frac{\partial f_{n+1}}{\partial \tau_n}d\tau_n + \frac{\partial r_{n+1}}{\partial r_n}d\lambda_n = 0 \,, \tag{15}$$

with

$$\frac{\partial f_{n+1}}{\partial \tau_n}d\tau_n + \frac{\partial r_{n+1}}{\partial r_n}d\lambda_n = 0 \,. \tag{16}$$

Fig. 4 schematizes the essential steps for the determination of the elastoplastic stress by the trapezoidal rule integration.

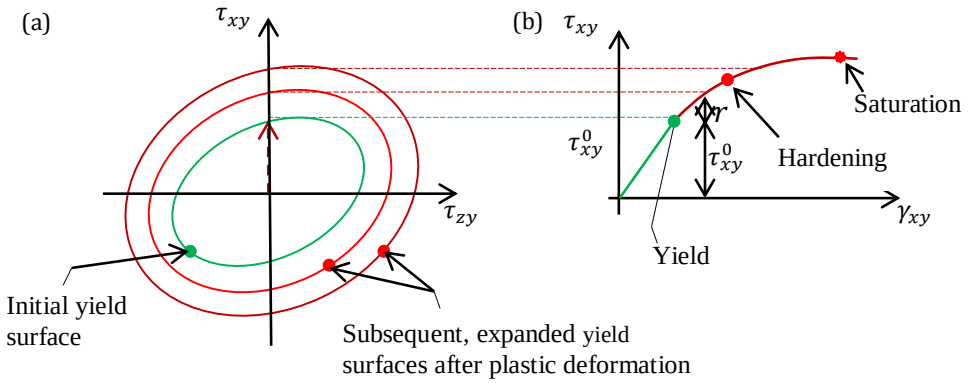

Fig. 3. (a) Isotropic hardening, in which the yield surface expands with plastic deformation; (b) the corresponding uniaxial stress-strain curve.

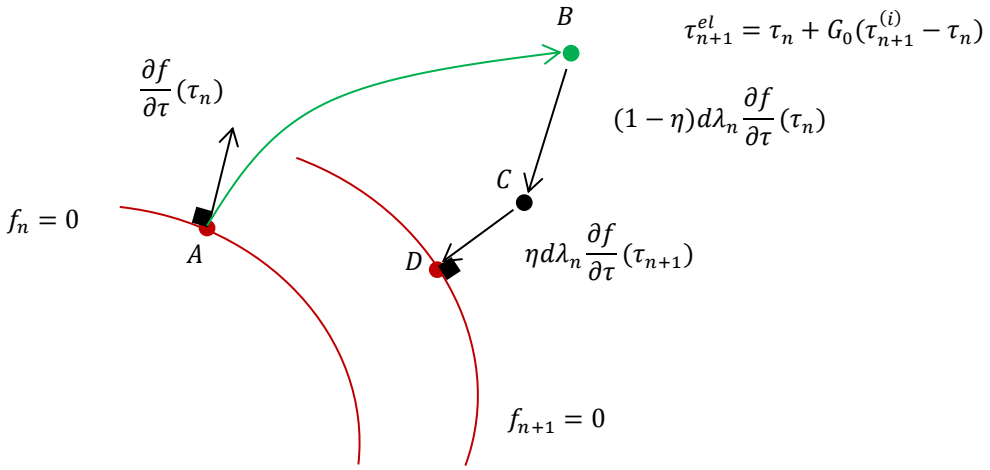

Fig. 4. Calculation of elastoplastic stress by a trapezoidal integration scheme.

According to Fig. 4, if $\eta = 0$ the diagram is the explicit Euler one, which generally requires a sub increment, and corrects at the end of the time. For $\eta = 0$, the implicit Euler method "Backward Euler" is placed. A first-order Taylor expansion about the point B in Fig. 4, *i.e.* (τ_{n+1}^{el}) gives

$$f_{n+1} = f_{n+1}^{el} + \frac{df_{n+1}^{T}}{d\tau_{n+1}^{el}} d\tau + \frac{df_{n+1}}{dr_{n+1}} dr = 0\,. \tag{17}$$

The total strain $d\varepsilon$ has already been applied in moving from point A to point B in Fig. 4, since $d\tau$ can be written as

$$d\tau = -d\lambda G_0 \left(\frac{df_{n+1}}{d\tau_{n+1}^{el}}\right). \tag{18}$$

Eq. (17) becomes

$$f_{n+1} = f_{n+1}^{el} - d\lambda \frac{df_{n+1}^{T}}{d\tau_{n+1}^{el}} G_0 \frac{df_{n+1}}{d\tau_{n+1}^{el}} - d\lambda H = 0\,. \tag{19}$$

The set of non-linear equations (17-19) is subsequently cast in a format of local residuals (in the sense that the residuals are defined at integration point level)

$$\begin{cases} r_\lambda = d\lambda - \left(\dfrac{f_{n+1}^{el}}{\frac{df_{n+1}^{T}}{d\tau_{n+1}^{el}} G_0 \frac{df_{n+1}}{d\tau_{n+1}^{el}} + H}\right) \\ r_\tau = \tau_{n+1} - \left(\tau_{n+1}^{el} - d\lambda G_0 \frac{df_{n+1}}{d\tau_{n+1}^{el}}\right) \end{cases}. \tag{20}$$

This system can be solved using an iterative procedure such *as Newton–Raphson* method (Bathe, 1996) to reduce r_λ and r_τ to (almost) zero while the final stresses should satisfy the yield criterion, $f_{n+1} = 0$. The term $-(1/d\lambda)(df/dr)dr$ is the hardening function H obtained to be the local slope of the uniaxial stress/plastic strain curve (Eq. (21)).

$$H = \frac{d\tau}{d\varepsilon^p} = \frac{G_T}{1 - \frac{G_T}{G_0}}, \tag{21}$$

For the unloading case, the elastoplastic tangent matrix is identical to the elastic matrix.

5. Results and Discussions

This section is dedicated to simulate the seismic behavior of a soil profile under the influence of various factors under seismic loading. The methodology developed in the present study is applied to a soil column of 5m thickness above bedrock with $G_{base} = 200$ MPa, and $\rho = 2000\,\mathrm{kg/m^3}$. Figs. 5 and 6 schematize the elastic linear strain-hardening stress-strain behavior for the uniaxial case, and shear modulus variation with depth, respectively.

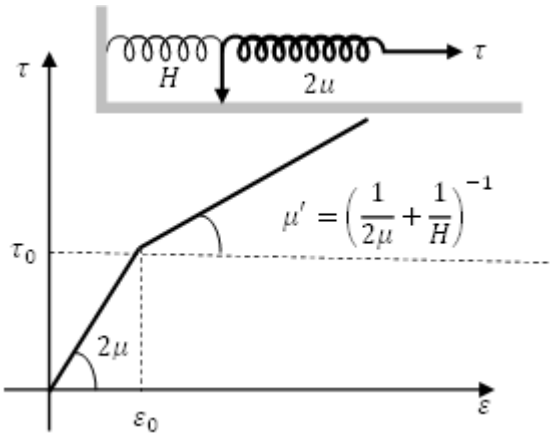

Fig. 5. Elastic, linear strain-hardening stress-strain behavior for the uniaxial case.

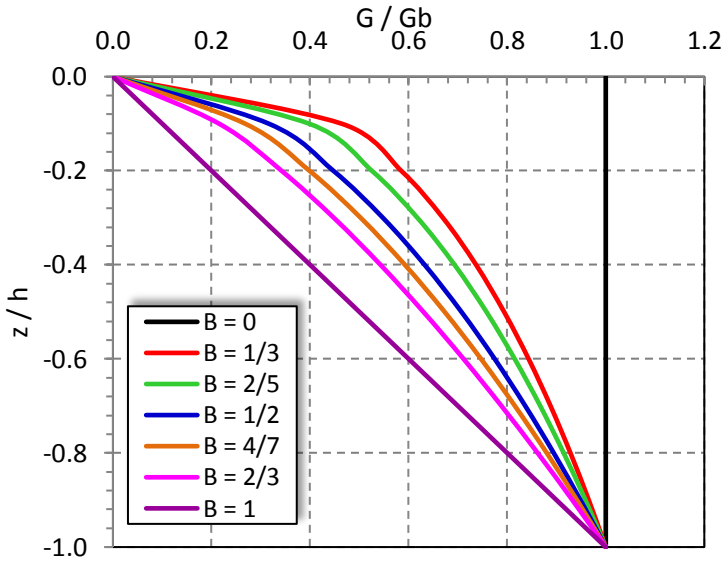

Fig. 6. Variation of shear modulus with depth.

The soil column is divided into five sublayers each one of 1m thickness. The response of the soil column is obtained in terms of depth-dependent displacements and accelerations as well as stress-strain hysteretic loop due to a vertical incident *SV* shear wave form the first order Ricker signal (Fig. 7).

Fig. 8 plots the depth-dependent distribution of maximum displacement along the soil column for different values of the parameter B in the nonlinear spatial variation of shear modulus. Fig. 9 shows the depth-dependent distribution of maximum acceleration with respect to that at the base of the soil profile (a_{max}/a_{base}). However Fig. 10 depicts the stress-strain hysteretic loop at the sublayer $n^{\circ}5$ due to the assumed degradation of shear modulus.

From Figs. 8 to 10, one may note the influence of the parameter B (power in the variation with depth of the shear modulus) on the predicted response. It expresses the key input step in the nonlinear response analysis of soils. On other hand, this shape of the hysteresis loop in Fig. 10 is controlled by its inclination and its breadth. The inclination of the loop depends on the stiffness (secant shear modulus) of the soil which decreases during the loading process. While the breadth of the hysteresis loop expresses the energy dissipation, commonly described by the damping ratio.

Another key parameter that controls the nonlinear response is the initial yield surface in terms of initial elastic strain as shown in Fig. 11(a) which depicts the depth-dependent distribution of maximum acceleration with respect to that at the base of the soil profile (a_{max}/a_{base}) for three assumptions of initial elastic strain. For the same assumptions, the stress-strain hysteretic loop is plotted in Fig. 11(b) at the level of the 5th sublayer.

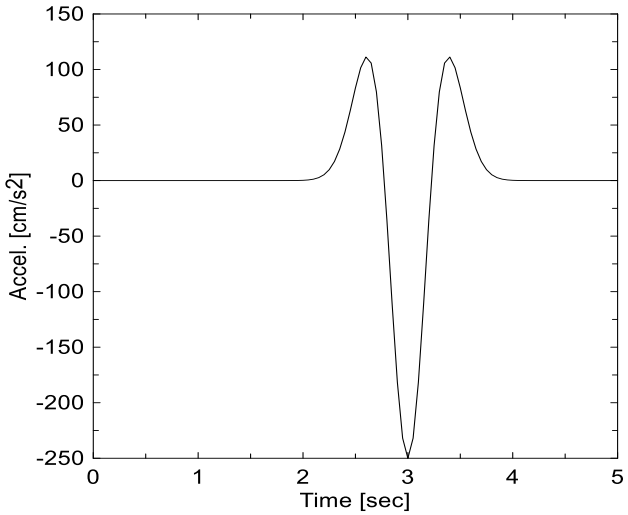

Fig. 7. Total acceleration time history at the base of the soil column.

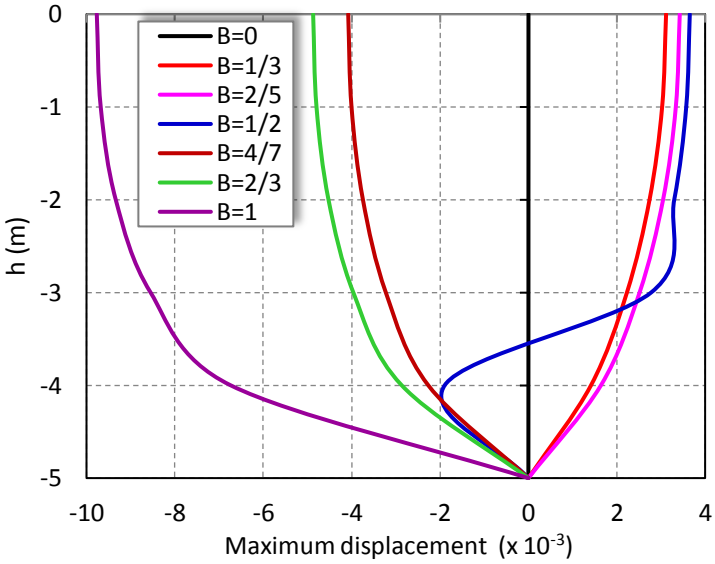

Fig. 8. Depth-dependent distribution of the maximum displacement along the soil profile.

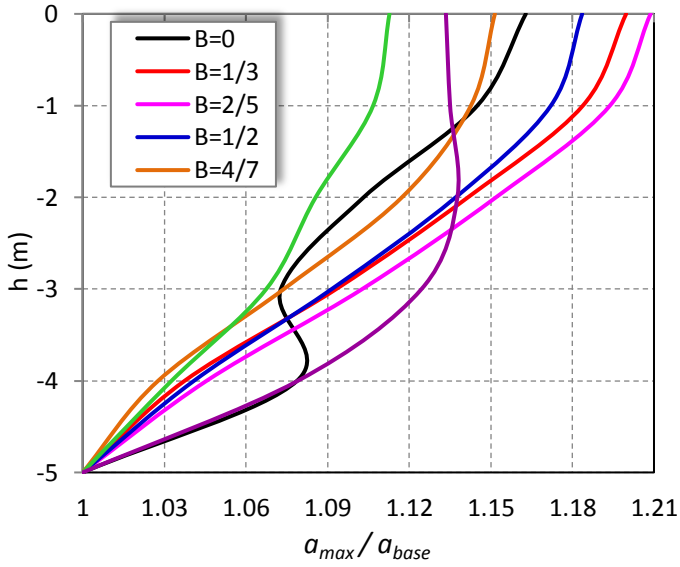

Fig. 9. Depth-dependent distribution of the maximum acceleration with respect to that at the base of the soil profile (a_{max}/a_{base}) along the soil profile.

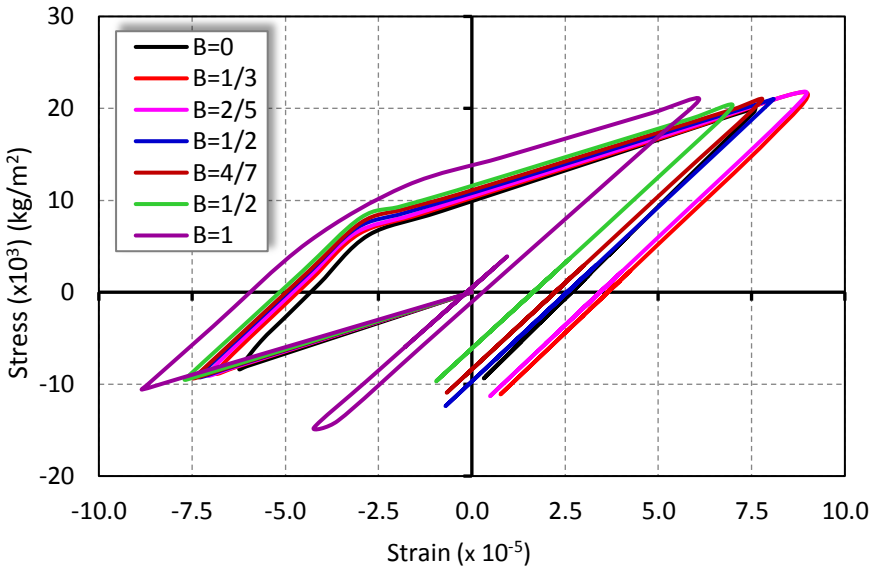

Fig. 10. Stress-strain hysteretic loop at sublayer number n°5.

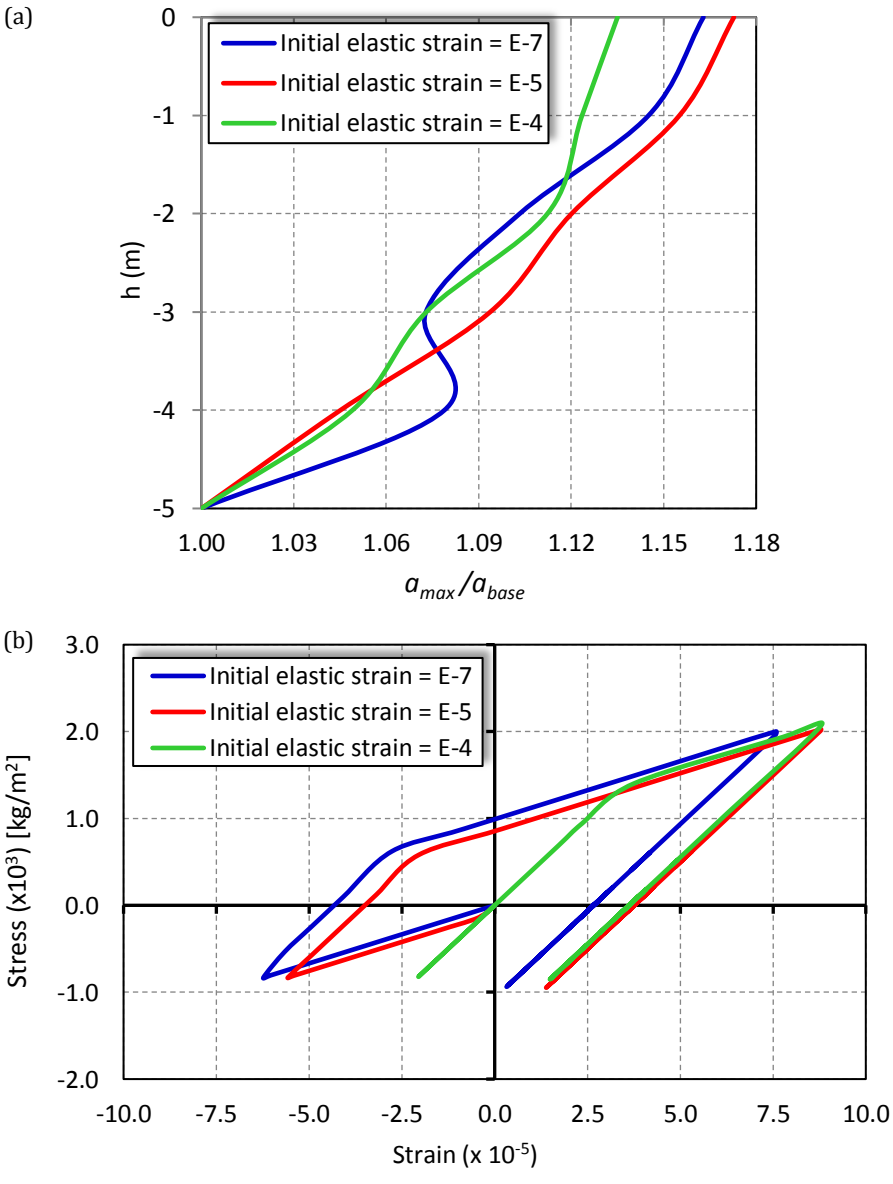

Fig. 11. Nonlinear responses of a soil profile for different initial yield surface: (a) ratio a_{max}/a_{base} ; (b) stress-strain hysteretic loop.

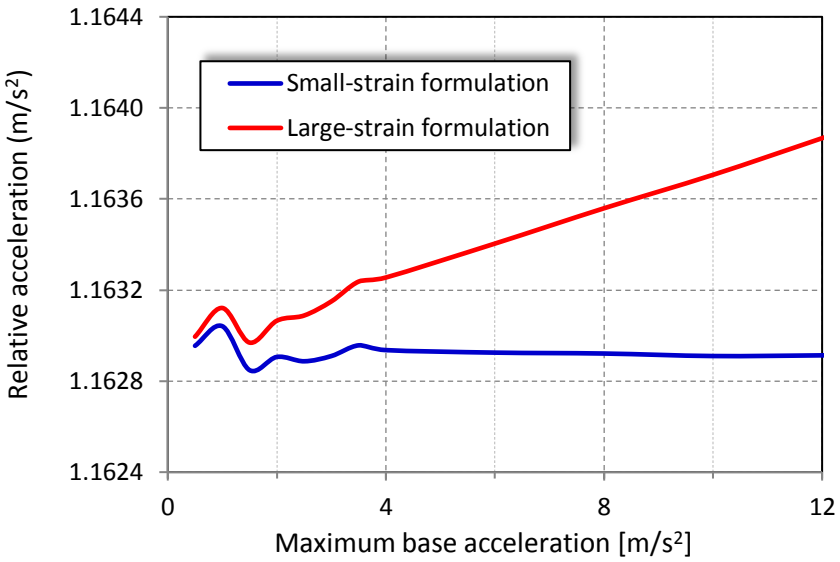

Fig. 12. Relative acceleration versus the maximum acceleration at the base of a soil profile for small- and large-strain formulations.

Under these conditions, both the inclination and the breadth of the loop are affected by the variation of the initial yield surface. So, to perfectly predict nonlinear soil responses, spatial variation of shear modulus together with material nonlinearity should be adequately selected according the each kind of material.

Finally, Fig. 12 shows the influence of the integration of the Von Mises elastoplastic equation according to small- and large-strain formulations. It compares the predicted soil responses in terms of relative accelerations of the soil profile versus maximal base acceleration using both small- and large-strain formulations. It is seen from Fig. 12, a large difference between the responses under the hypotheses of small- and large-strain formulations when the base acceleration (excitation) increases. However, deep interpretation of such behavior needs appropriate selection of the calculation method according to the solicitation level in the loading process, especially in the cases of seismic shaking.

6. Conclusions

The present study was principally dedicated to the development of a methodology to incorporate spatial and material variation of shear modulus in predicting the nonlinear responses of soil deposits under seismic excitations according to the incremental theory of plasticity. Moreover, the efficiency of the elastoplastic model using the Von Misès criterion in the prediction of the seismic responses was studied.

Firstly, the problem was formulated under the assumption of isotropic hardening in which the yield surface expands with plastic deformation, in the formwork of the FEM. Then, the equation of motion was integrated using the Newmark integration scheme. Lastly, a parametric study was conducted to show the influence of some parameters on the predicted responses.

This study showed that several factors considerably influence the nonlinear predicted seismic ground responses. The variation of the stiffness matrix due to the variation of the parameter B translating the spatial variation of the shear modulus leaded to large variations in the predicted nonlinear soil profile response in terms of depth-dependent distribution of the maximum displacement (Fig. 8) along the soil profile, maximum depth-dependent distribution of the maximum acceleration with respect to that at the base of the soil profile (Fig. 9), and stresses-strain hysteretic loop (Fig. 10). Also, the initial elastic strain affected the predicted responses (Fig. 11(a,b) because the evolution of the yield surface depends on these limits. Finally, the calculation method, i.e. small- or large-strain formulation also guided the predicted responses (Fig. 12).

So, accurate prediction of nonlinear seismic soil responses should adequately include spatial variation of soil properties such as shear modulus together with material nonlinearity for soil material. Furthermore, appropriate constitute equation and efficient integration scheme are required.

There is also the option to include a subheading within the Appendix if you wish.

References

Abdel-Ghaffar A, Koh AS (1981). Longitudinal vibration of non-homogeneous earth dams. *Earthquake Engineering and Soil Dynamics*, 9(3), 279-305.

Afra H, Pecker A (2002). Calculation of free field response spectrum of a nonhomogeneous soil deposit from bed rock response spectrum. *Soil Dynamics and Earthquake Engineering*, 22(2), 157–65.

Bathe KJ (1996). Finite Element Procedures. Library of Congress Cataloging-in-Publication Data.

Chopra A (2012). Dynamics of structures: Theory and applications to earthquake engineering. Prentice Hall.

Dakoulas P, Gazetas G (1985). A class of inhomogeneous shear models for seismic response of dams and embankments. *Soil Dynamics and Earthquake Engineering*, 4, 166-182.

Dunne F, Petrinic N (2006). Introduction to computational plasticity. Oxford University Press.

Elgamal AW (1991). Shear hysteretic elasto-plastic earthquake response of soil systems. *Earthquake Engineering and Structural Dynamics*, 20(4), 371-387.

Gu Q, Conte J P, Elgamal A, Yang Z (2009). Finite element response sensitivity analysis of multi-yield-surface J2 plasticity. *Computer Methods in Applied Mechanics and Engineering*, 198(30–32), 2272–2285.

Harichane Z, Chehat A, Sadouki A (2011a). Viscoelastoplastic earthquake shear hysteretic response of geomaterials. *Electronic Journal of Geotechnical Engineering*, 16 (Bund. M), 1566 -1582.

Harichane Z, Chehat A, Afra H (2011b). Post-elastic behavior of soil profiles under earthquake excitations. *Electronic Journal of Geotechnical Engineering*, 16 (Bund. P), 1471 -1485.

Harichane Z, Afra H, Bahar R (2012). Experimental validation of an identification procedure of soil profile characteristics from free field acceleration records. *International Journal of Geotechnical Earthquake Engineering*, 3(1), 1-17.

Hashash YMA, Park D (2001). Non-linear one-dimensional seismic ground motion propagation in the Mississippi embayment. *Engineering Geology*, 62(1–3), 185–206.

Hashash YMA, Park D (2002). Viscous damping formulation and high frequency motion propagation in non-linear site response analysis. *Soil Dynamics and Earthquake Engineering*, 22, 611-624.

Kaklamanos J, Baise LG, Thompson EM, Dorfmann L (2015). Comparison of 1D linear, equivalent-linear, and nonlinear site response models at six KiK-net validation sites. *Soil Dynamics and Earthquake Engineering*, 69, 207-219.

Khellafi MA, Harichane Z, Afra H, Sadouki A (2013). A case study of accelerometric records analysis of May 21st, 2003, Boumerdes (Algeria) earthquake. *International Journal of Geotechnical Earthquake Engineering*, 4(2), 34-52.

Mercado V, El-Sekelly W, Zeghaland M, Abdoun T (2015). Identification of soil dynamic properties through an optimization analysis. *Computers and Geotechnics*, 65, 175–186.

Pecker A (1995). Validation of small strain properties from recorded weak seismic motions. *Soil Dynamics and Earthquake Engineering*, 14(6), 399–408.

Stewart JP, Kwok AOL, Hashash YMA, Matasovic N, Pyke R, Wang Z, Yang Z (2008). Benchmarking of nonlinear geotechnical ground response analysis procedures. PEER Report 2008/04, University of California, Berkeley.

Vasileiois AD, Georolymos N, Gazetas G (2012). Constitutive model for soil amplification of ground shaking: Parameter calibration, comparisons, validation. *Soil Dynamics and Earthquake Engineering*, 42, 255–274.